Spin anisotropy in Cu(*en*)$(H_2O)_2SO_4$: A quasi-two-dimensional $S = 1/2$ spatially anisotropic triangular-lattice antiferromagnet

R. Tarasenko,[1] A. Orendáčová,[1,*] E. Čižmár,[1] S. Maťaš,[2] M. Orendáč,[1] I. Potočňák,[3] K. Siemensmeyer,[2] S. Zvyagin,[4] J. Wosnitza,[4] and A. Feher[1]

[1]*Institute of Physics, Faculty of Science, P. J. Šafárik University, Park Angelinum 9, SK-041 54 Košice, Slovak Republic*

[2]*Helmholtz-Zentrum Berlin, Hahn-Meitner-Platz 1, D-14109 Berlin, Germany*

[3]*Institute of Chemistry, Department of Inorganic Chemistry, Faculty of Science, P. J. Šafárik University, Moyzesova 11, SK-041 54 Košice, Slovak Republic*

[4]*Dresden High Magnetic Field Laboratory (HLD), Helmholtz-Zentrum Dresden-Rossendorf and TU Dresden, D-01314 Dresden, Germany*

(Received 14 March 2013; published 1 May 2013)

We have studied in detail the effect of the spin anisotropy on the electron paramagnetic resonance spectra and magnetic properties of Cu(*en*)$(H_2O)_2SO_4$, an $S = 1/2$ spatially anisotropic triangular lattice antiferromagnet. The angular and temperature dependence of the resonance fields as well as the magnetization and magnetic susceptibility reflect the exchange and g-factor anisotropy with $J_z/J_{x,y} < 1$ and $g_z/g_{x,y} > 1$, respectively. The exchange anisotropy and Dzyaloshinskii-Moriya interaction are responsible for the main broadening mechanism at higher temperatures while spin-diffusion effects prevail at helium temperatures. The ratio of the uniform susceptibilities calculated along the three crystal directions suggests an easy-axis anisotropy with the a axis as the magnetic easy axis. Its impact on the physical properties of the title compound is discussed.

DOI: 10.1103/PhysRevB.87.174401 PACS number(s): 75.30.Gw, 75.30.Cr, 75.40.Cx, 75.50.Ee

I. INTRODUCTION

Two-dimensional quantum magnets provide a fruitful playground for the research of ordering phenomena and new quantum states resulting from the interplay of quantum fluctuations and magnetic anisotropy.[1,2] One example of such states is the quantum spin liquid. The existence of spin continua in Cs_2CuCl_4 has been attributed to the proximity of the system to the quantum-spin-liquid state in which spin-wave excitations are fractionalized into spin-1/2 spinons.[3] The observation prompted intensive theoretical investigations to search for the existence of the spin-liquid state in the $S = 1/2$ spatially anisotropic triangular lattice (SATL) with antiferromagnetic Heisenberg interactions J_1 and J_2 (Refs. 4–6). The model described by the Hamiltonian

$$H = J_1 \sum_{i,j} S_i S_j + J_2 \sum_{i,k} S_i S_k \qquad (1)$$

interpolates between the unfrustrated square lattice with a collinear Néel order ($J_2 = 0$), fully frustrated triangular lattice ($\alpha = J_2/J_1 = 1$), and decoupled chains ($J_1 = 0$). The indices i, j, and k refer to the nearest-neighbor and next-nearest neighbor spins, respectively.

A variety of different kinds of disordered ground states have been reported for this rather simple model.[4,7,8] While the existence of a spiral Néel state has been established around the isotropic point for the $1 \leqslant \alpha \leqslant 1.4$ region,[9] the ground states of more anisotropic regions are still under debate.[8–10]

A spin anisotropy, always present in real systems, can change essentially ground-state properties of isotropic models. The introduction of an easy-plane spin anisotropy in the SATL leads to the stabilization of the spiral Néel phase over a wide region of α (Ref. 11). The Dzyaloshinskii-Moriya (DM) interaction has a similar effect on the stabilization of the spiral phase in the SATL for large α (Refs. 12 and 13). The effect of an easy-axis anisotropy on the ground-state properties of the SATL has been investigated in detail only for the limiting cases ($\alpha = 0$ and 1).[14–16] Recently, a proximity to the quantum-spin-liquid state has been proposed for $Ba_3CoSb_2O_9$—a triangular-lattice antiferromagnet with an effective spin 1/2 and a weak easy-axis anisotropy, where an extensive inelastic neutron-scattering continuum above spin-wave excitations has been observed in the ordered phase.[17]

Cu(*en*)$(H_2O)_2SO_4$ (en = ethylendiamine = $C_2H_8N_2$) has been previously identified as a potential candidate for a SATL with $\alpha \ll 1$ and an effective antiferromagnetic intralayer exchange coupling $J/k_B = 2.8$ K (Ref. 18). The effective coupling J is related to the average of the interactions J_1 and J_2 in the Hamiltonian (1). The system undergoes a phase transition to the ordered state at $T_C = 0.91$ K. A frustration ratio $f = |\theta|/T_C \approx 4$, where θ represents the paramagnetic Curie temperature, indicates a rather weak frustration, as can be expected for the collinear Néel phase.

Specific-heat studies in magnetic fields $B < B_{sat} \approx 7$ T reveal a nonmonotonic shift of the transition temperature[19]—a typical feature of a field-induced Berezinskii-Kosterlitz-Thouless (BKT) phase transition[20] which can be preserved in real two-dimensional (2D) magnets with a sufficiently weak interlayer coupling J' (Ref. 21). Apparently, Cu(*en*)$(H_2O)_2SO_4$ with $|J'/J| \approx 0.003$ meets this requirement. Quantum Monte Carlo studies of layered Heisenberg magnets provide a critical value of the ratio, $|J'/J| \approx 0.01$, below which a specific-heat anomaly associated with the three-dimensional (3D) ordering vanishes.[22] Correspondingly, the pronounced λ-like anomaly observed in Cu(*en*)$(H_2O)_2SO_4$ (Ref. 18) might result from the interplay of the interlayer coupling and other mechanisms such as magnetic anisotropy.[14,23]

The main motivation of this work was the exploration of the spin anisotropy in the quasi-two-dimensional spatially anisotropic triangular-lattice Heisenberg antiferromagnet Cu(*en*)$(H_2O)_2SO_4$. We first describe the crystal structure and experimental details, followed by the presentation and discussion of the experimental results. This includes the analysis of powder neutron diffraction, electron paramagnetic

resonance spectra, single-crystal magnetization, and static susceptibility. Possible consequences of the spin anisotropy for the ground-state properties of Cu(*en*)$(H_2O)_2SO_4$ are discussed. The paper concludes with a summary and some comments about possible future directions.

II. STRUCTURAL AND EXPERIMENTAL DETAILS

The crystal structure of Cu(*en*)$(H_2O)_2SO_4$ determined at 300 K is monoclinic, space group $C2/c$ with the unit cell parameters $a = 7.232$ Å, $b = 11.725$ Å, $c = 9.768$ Å, $\beta = 105.50°$, and $Z = 4$ (Ref. 24). The structure consists of neutral covalent chains running along the crystallographic a axis which are linked by hydrogen bonds along the b and c axes (Fig. 1). Cu(II) ions are located in the center of a distorted octahedron elongated along the a axis with the bond lengths in the equatorial plane d(Cu–O1), d(Cu–O2) = 1.964 Å, and d(Cu–N1), d(Cu–N2) = 1.979 Å and the apical positions d(Cu–O5) = 2.494 Å. The octahedrons within the ab plane have the same orientation while a rotation by 180° appears along the c axis due to the inversion center located in the center of the unit cell (Fig. 1).

The absence of an inversion center between pairs of nearest-neighbor Cu(II) ions within the ab plane (in Fig. 1 denoted as 1, 2, 3 or 1′, 2′, 3′) allows for the antisymmetric Dzyaloshinskii-Moriya interaction $\vec{d}_{i,j} \cdot (\vec{S}_i \times \vec{S}_j)$, where $\vec{S}_{i,j}$ denotes the spins of the ith and jth Cu(II) ion and $\vec{d}_{i,j}$ is the DM vector. Following Moriya's symmetry rules[25] the DM vectors $\vec{d}_{1,3}, \vec{d}_{1,2}, \vec{d}_{2,3}$ should be nonzero. No DM coupling is expected between the atoms from neighboring ab planes, i.e., $\vec{d}_{i,j} = 0$ where $i = 1, 2, 3$ and $j = 1', 2', 3'$. The strength of the DM interaction depends on the exchange coupling between the mentioned pairs of atoms. Previous studies[18] identified the ab plane as the magnetic layer, thus DM coupling can be expected.

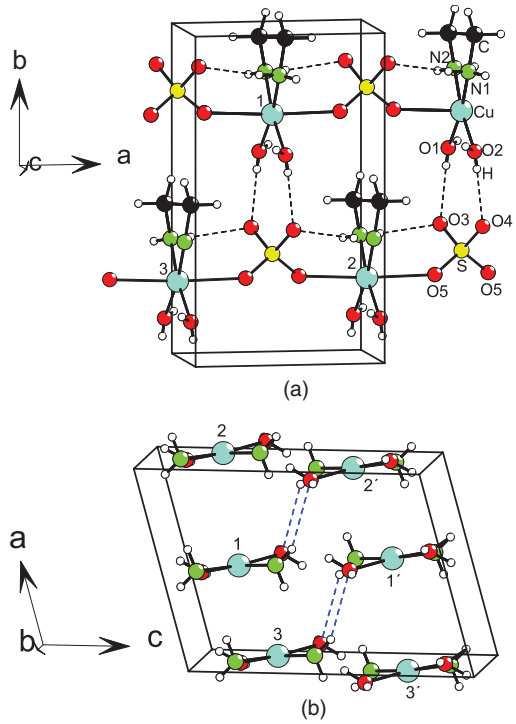

FIG. 1. (Color online) (a) Crystal structure of Cu(*en*)$(H_2O)_2SO_4$ projected to the ab plane. (b) Projection of the crystal structure to the ac plane. The $[SO_4]^{2-}$ anions are omitted for the sake of clarity. The dashed lines represent hydrogen bonds. The numbers 1, 2, 3, and 1′, 2′, 3′ denote the individual Cu(II) ions in the unit cell.

Cu(*en*)$(H_2O)_2SO_4$ single crystals were prepared in the form of blue elongated plates using a modified method as published in the Ref. 24. Deuterated polycrystals were grown as well stored in the nitrogen atmosphere for further use.

Powder neutron diffraction studies were performed at Helmholtz-Zentrum Berlin using the powder diffractometer E6 equipped with the VM-1 magnet and ^{3}He-insert. A deuterated polycrystalline sample of total mass of 1.6 g was powdered, pressed into a pellet, and stored in a copper can filled with ^{3}He exchange gas to improve the thermal contact between the sample and surrounding. Diffraction patterns were collected with a long counting time at several temperatures between 0.4 and 40 K in zero magnetic field using an incident-neutron wavelength $\lambda = 2.45$ Å. The patterns were analyzed with Rietveld method using the software package FULLPROF.[26]

Electron paramagnetic resonance (EPR) measurements were performed at the Dresden High Magnetic Field Laboratory using an X-band spectrometer (Bruker ELEXSYS E500) at a fixed frequency of 9.4 GHz in the temperature range from 2 to 300 K and magnetic fields up to 0.5 T. A single crystal with the approximate dimensions $a' \times b' \times c' = 2 \times 0.7 \times 0.5$ mm^3 was glued on a Suprasil-quartz rod. The angular dependence of the EPR spectra was investigated by rotating the crystal within the $b'c'$, $a'c'$, and $a'b'$ planes.

Magnetization and static-susceptibility measurements were performed in a commercial superconducting quantum interference device (SQUID) magnetometer. A single crystal with a mass of 45 mg and dimensions $10 \times 3.6 \times 0.9$ mm^3 was used for the bulk measurements. Using standard Pascal constants, the susceptibility data were corrected for the core diamagnetism.

III. RESULTS AND DISCUSSION

A. Neutron diffraction

Recent comparative magnetostructural studies of Cu(*en*)$(H_2O)_2SO_4$ and its deuterated analog Cu(d-*en*)$(D_2O)_2SO_4$ revealed only a slight reduction of the exchange interactions[27] in accordance with the negligible structural differences observed at room temperature.[28] The analysis of the neutron diffraction patterns of the deuterated analog (Fig. 2) confirmed the preservation of the monoclinic space group $C2/c$ symmetry down to the lowest temperatures. The rather significant contraction observed for the c lattice parameter below 40 K can be ascribed to hydrogen-bonding effects (Fig. 2, inset). Such significant changes were observed in other Cu(II) materials where the hydrogen bonding plays an important role in controlling both the long-range and local structure. It was found that the pronounced effect of the hydrogen-bonding interactions appeared below nitrogen temperatures.[29]

It should be noted that the diffraction pattern recorded at 0.45 K, well below the ordering temperature, does not contain any additional Bragg reflections arising from the scattering

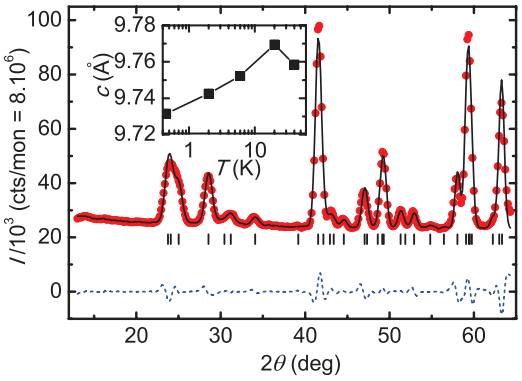

FIG. 2. (Color online) Diffraction pattern of Cu(d-*en*)$(D_2O)_2SO_4$ collected at 0.45 K. Circles represent measured data, the solid line is the calculated pattern fitted to the data. The vertical lines indicate the position of Bragg nuclear reflections and the dashed line represents the difference between the data and the calculated pattern. Inset: Temperature evolution of Rietveld refined c-lattice parameter of Cu(d-*en*)$(D_2O)_2SO_4$.

on the ordered magnetic moments of the Cu(II) ions. The absence of forbidden reflections in the powder experiment can be attributed to a weak magnetic signal and to the extremely high incoherent scattering due to the presence of hydrogen atoms in the structure. Both facts lead to a very unfavorable signal to background ratio.

B. EPR resonance fields and g factor

The EPR spectra investigated in the paramagnetic phase above 2 K consist of a narrow single resonance line in all orientations and temperatures. The resonance lines were fitted to a Lorentzian formula with two fit parameters, the resonance field B_r $(=\mu_0 H_r)$ and the linewidth ΔB. The former was used for the calculation of g factors applying the resonance condition $\hbar\omega = g\mu_B B_r$. The angular dependence of the g factor was fitted using the standard relation

$$g^2 = g_z^2 \cos^2\theta + g_x^2 \sin^2\theta \cos^2\varphi + g_y^2 \sin^2\theta \sin^2\varphi, \qquad (2)$$

where g_x, g_y, and g_z are the g factors corresponding to the local anisotropy axes x, y, and z defining the principal axes of the g tensor. θ is the angle between the magnetic field and the local z axis and φ is the angle between the projection of the magnetic field in the xy plane and the local x axis.

A few crystals were used for a room-temperature x-ray study to determine the orientation of the crystallographic axes a, b, and c with respect to the crystal edges a', b', and c'. The longest crystal edge a' was identified with the crystallographic a axis and the shortest crystal edge c' is parallel to the b axis. The local-anisotropy axes were chosen considering the octahedral coordination of the Cu(II) ion; the local z axis was identified with the a axis and the xy plane—the equatorial plane of the octahedron, was identified with the $b'b$ plane, in which the local x axis is tilted by 45° from the b axis [Fig. 3(a)].

The extremal values of the g factor found within the $b'b$ plane do not coincide with the choice of the principal axes of the g tensor; the maximum and minimum values were found along the b' and b axes, respectively [Fig. 3(b)]. The observed shift together with a vanishing difference between the

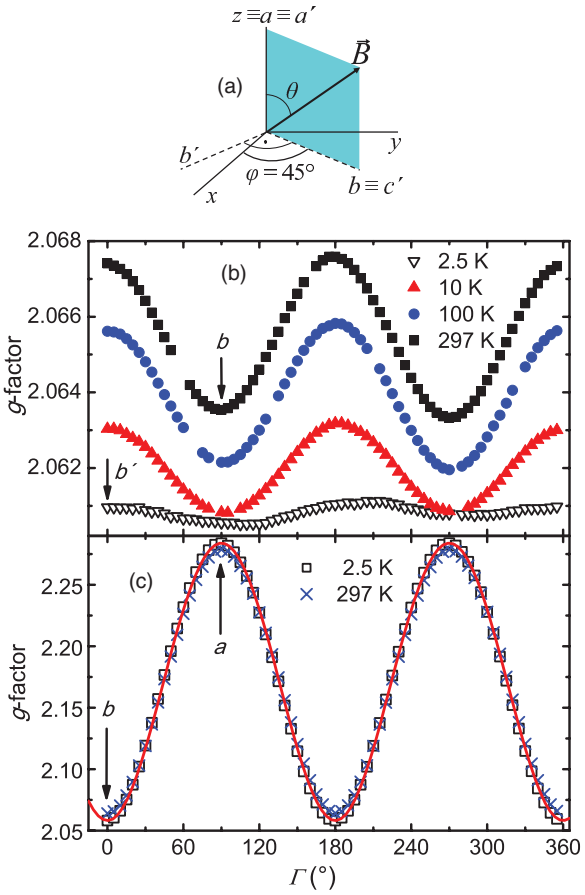

FIG. 3. (Color online) (a) Coordinate system of the local anisotropy axes x, y, and z. (b) Angular variation of the g factor of Cu(*en*)$(H_2O)_2SO_4$ in the $b'b$ plane at various temperatures. (c) Angular variation of the g factor of Cu(*en*)$(H_2O)_2SO_4$ in the ab plane. For clarity, only data at selected temperatures are shown. The solid line represents the fit to Eq. (2) performed for the data at $T = 2.5$ K.

extremal g values at low temperatures suggest a partial mixing of the g_z component resulting from a slight deformation of the octahedron (Fig. 1). Correspondingly, the axes of the chosen coordinate system can deviate from the actual one by a few degrees. Therefore, the analysis of the angular variation of the g factor was performed in the ab plane, where the angular change is dominated by a θ dependence [Fig. 3(c)]. A deviation from the actual orientation of the g tensor was taken into account by corrections to the polar angles introduced as free fit parameters p_θ, p_φ. Denoting Γ as angle of crystal rotation, the relations $\theta = \Gamma + p_\theta$ and $\varphi = p_\varphi$ were used in Eq. (2). We found the nearly temperature-independent parameters $p_\theta = (90 \pm 0.5)^\circ$ and $p_\varphi = (45 \pm 1)^\circ$ which support the choice of the coordinate system as depicted in Fig. 3(a).

Fits of the g-factor variation within the ab plane at different temperatures yield the temperature dependence of g_x, g_y, and g_z as shown in Fig. 4. To check the reliability of the obtained results, we studied in a separate experiment the temperature dependence of the resonance field with magnetic field applied along the a and b axes. The corresponding g_b factors lie between the g_x and g_y factors and g_a follows the temperature dependence of g_z. A systematic shift $\Delta g = g_a - g_z \approx 0.002$ in the whole temperature region can be ascribed to a slight

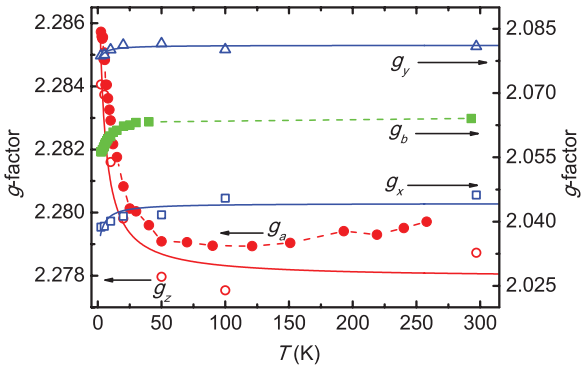

FIG. 4. (Color online) Temperature dependence of g factors in $Cu(en)(H_2O)_2SO_4$ obtained from the analysis of the g-factor variation within the ab plane (open symbols). The full symbols represent the g_a and g_b values obtained in a separate experiment. The solid lines represent fit curves obtained by the fitting to Eq. (5). The dashed lines are guides for eyes.

(within a few degrees) crystal misorientation and/or the already mentioned deviations of the coordinate system.

At low temperatures, the temperature dependence of g_z is opposite to that observed for g_x and g_y. Such a behavior has experimentally been observed in other low-dimensional magnets[30–33] and agrees with theoretical predictions for the resonance fields in the presence of dipolar coupling and exchange anisotropy.[30–32,34] Both interactions represent spin-symmetric perturbation terms in the spin Hamiltonian

$$H'_S = \sum_{i,j} S_i \bar{\bar{J}} S_j, \tag{3}$$

where $\bar{\bar{J}}$ denotes a tensor of the anisotropic interaction between the ith and jth spin resulting from both, the dipolar coupling H'_{DD} and the exchange anisotropy H'_{AE}. For antisymmetric spin perturbations H'_{A}, such as the DM interaction, it was shown that they influence the resonance frequency of one-dimensional magnets only for a DM vector parallel to the chain axis.[30]

A look at the temperature dependence of the g factors in Fig. 4 suggests the presence of at least dipolar and anisotropic exchange interactions in $Cu(en)(H_2O)_2SO_4$. Considering the H'_{AE} and H'_{DD} terms, the relation between the resonance field B_{res} and resonance frequency ω has been derived for $B \parallel z$ (Ref. 31) as

$$\hbar\omega_z = g_z^0 \mu_B B_{\mathrm{res}}^z \left[1 - \frac{\chi_z(T)}{N g_z^2 \mu_B^2}(2J_{zz} - J_{xx} - J_{yy})\right], \tag{4}$$

where χ_z(T) is the susceptibility, g_z^0 represents the high-temperature value of g_z, and the J's are diagonal terms of the $\bar{\bar{J}}$ tensor. Analogous expressions for $B \parallel x$ and $B \parallel y$ can be obtained by changing (x, y, z) into (y, z, x) and (z, x, y), respectively. Assuming a fixed microwave frequency and sufficiently high temperatures, where χ(T) can be approximated by a Curie-Weiss law, Eq. (4) transforms

$$g_z(T) = g_z^0 \left[1 - \frac{S(S+1)}{3(T-\theta)} \cdot \frac{K_z}{k_B}\right]. \tag{5}$$

The parameter K_z is the aforementioned combination of J's. By use of this equation and taking $\theta = -3.3$ K from Ref. 18, we obtained the fit lines shown in Fig. 4. The fits yield the high-temperature values $g_x^0 = 2.044$, $g_y^0 = 2.081$, $g_z^0 = 2.278$ as well as the estimates of the effective spin-anisotropy parameters $J_{xx}/k_B = 0.021$ K, $J_{yy}/k_B = -0.003$ K, and $J_{zz}/k_B = -0.026$ K. The sum of the parameters is close to zero as expected for the trace of an anisotropic exchange tensor. As was shown in Ref. 25, the order of magnitude of the exchange anisotropy is given by $|J^{\mathrm{AE}}| \approx (\Delta g/g)^2\,|J|$, where J is an isotropic coupling and Δg is the deviation from the free-electron value. Using $g = 2.134$, the average value of the high-temperature g factors, and $J/k_B = 2.8$ K, the estimate of the exchange anisotropy $|J^{\mathrm{AE}}|/k_B = 0.011$ K agrees well with the average value of above $|J_{ii}|$'s $(i = x, y, z)$, namely, $\langle|J_{ii}|/k_B\rangle = 0.017$ K.

The spin anisotropy introduced by dipolar coupling between adjacent spins, separated by the distance r within the ab plane, can be estimated by $J_{ii}^{\mathrm{DD}} = \frac{\mu_0 \mu_B^2 g_i^2}{4\pi k_B r^3}(1 - \frac{3r_i^2}{r^2})$, where r_i represents the components of the position vector $\vec{r}$. Using the coordinates of the adjacent Cu(II) ions 1, 2, and 3 (Fig. 1) the shortest distances are $r_{23} = 7.145$ Å and $r_{21} = 6.840$ Å. The anisotropic coupling between the Cu pairs (2, 3) and (2, 1) then leads to the average value $\langle|J_{ii}^{\mathrm{DD}}|/k_B\rangle = 0.011$ K, which agrees well with $|J^{\mathrm{AE}}|/k_B$. This suggests, that despite rather long distances between the Cu ions, dipolar coupling provides an important contribution to the spin anisotropy in $Cu(en)(H_2O)_2SO_4$. Theoretical and experimental studies of the contributions J^{DD} and J^{AE} in low-dimensional Cu(II) compounds revealed that J^{AE} can be comparable to J^{DD} (Ref. 35). Finally, the anisotropic exchange couplings $J_i = J + J_{ii}$ evaluated using $J/k_B = 2.8$ K and the J_{ii}'s found above indicate an easy-plane anisotropy with the lowest value J_z along the a direction.

C. Temperature and angular dependence of the EPR linewidth

The angular dependence of the linewidth was investigated in the ab and $b'b$ planes. The angular dependence in the ab plane changes significantly with temperature [Fig. 5(a)]. At lowest temperatures, when 2D antiferromagnetic short-range order becomes relevant, alternating small and large maxima appear, typical for the $(3\cos^2\theta_{\mathrm{m}}\text{-}1)^2$ dependence resulting from spin-diffusion processes in two-dimensional magnets with weak interlayer coupling.[36,37] Here, θ_{m} represents the angle between the magnetic field and the normal to the magnetic layer. Apparently, the observed angular dependence indicates the rotation of the magnetic field out of the magnetic layer.

With increasing temperature, the small and large peaks gradually merge together forming one wide maximum with a period of 180° resembling a simple $\cos^2\theta$ dependence of the g factor (Fig. 3). For non-S-state ions such as Cu(II), spin anisotropies are the dominant contribution to the second moment due to a large spin-orbit coupling, possibly leading to the $\cos^2\theta$ dependence of the linewidth.[36,38,39] Previous studies indicated rather weak interlayer coupling in $Cu(en)(H_2O)_2SO_4$. Thus the contributions from both spin anisotropy and spin-diffusion processes can be expected.

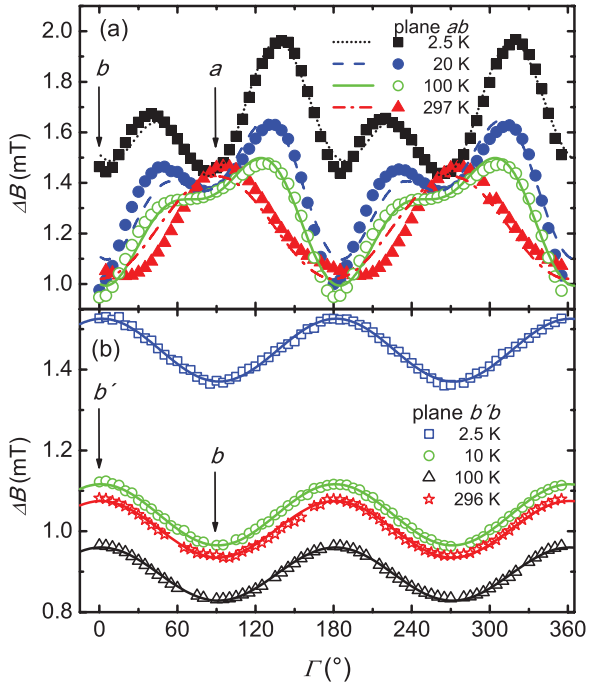

FIG. 5. (Color online) (a) Angular dependence of the EPR linewidth in the *ab* plane studied at constant temperatures. The lines represent fit curves obtained by use of Eq. (8). (b) Angular dependence of the linewidth in the $b'b$ plane studied at constant temperatures. The solid lines represent fit curves obtained by use of Eq. (6). For clarity, only data obtained at selected temperatures are shown.

The linewidth within the $b'b$ plane follows at all temperatures an angular dependence, which indicates a dominant spin-anisotropy contribution [Fig. 5(b)]. The absence of double maxima suggests that not the previously expected *ab* plane,[18] but the $b'b$ plane is identified as the magnetic layer with the normal parallel to the *z* axis. Using theoretical predictions for the contribution of the symmetric anisotropic exchange and antisymmetric exchange to the second moment, M_2^{S} and M_2^{A}, respectively,[36,38] the simplified relation

$$\Delta B = A + B\cos^2\varphi \tag{6}$$

has been derived when assuming a coincidence of the principal axes of the DM vector, $\bar{\bar{J}}$, and $\bar{\bar{g}}$ tensors. Here, $\theta = \theta_{\mathrm{m}} = \pi/2$ and $\varphi = \Gamma + \delta$. Γ is the angle of rotation within the $b'b$ plane and δ is a free parameter involving a potential deviation from the chosen coordinate system of the $\bar{\bar{g}}$ tensor. Under these conditions, the second term in Eq. (6) stands for the M_2^{A} contribution while the first term involves the contribution of M_2^{S} and spin-diffusion processes. The fit procedure provides nearly identical results for δ being either $0^\circ \pm 2^\circ$ or $90^\circ \pm 2^\circ$ [Fig. 5(b)]. The deviation of the parameter δ from 45° suggests a different coordinate system for the DM vector, which cannot be simply determined when applying Moriya's symmetry rules.

To obtain a proper formula for the analysis of the angular variation of the linewidth within the *ab* plane, the coordinate system for the DM vector has been rotated by 45° around the *z* axis, then angle $\varphi = 0^\circ$ (equivalent to the choice $\varphi = 90^\circ$) was fixed and $\theta = \theta_{\mathrm{m}} = \Gamma + \pi/2$. The resulting formula was applied in the form[36,38]

$$\Delta B = A^* + B^*\cos^2\theta + C^*(3\cos^2\theta - 1)^2, \tag{7}$$

where the second term contains both M_2^{S} and M_2^{A} contributions.

This equation does not yield a reasonable agreement with the experimental data even at 2.5 K, where the third term in Eq. (7) prevails. The deviations could be attributed to the simplified choice of the magnetic layer. Thus, a detailed analysis of potential magnetic layers was performed in the following way: all possible layers were constructed by the combinations of the arbitrary three ions within the unit cell. For each layer, a separate transformation $\theta_{\mathrm{m}}(\Gamma)$ has been derived and the corresponding angular variation of the linewidth has been calculated using the simplified relation $A^* + C^*[3\cos^2\theta_{\mathrm{m}}(\Gamma) - 1]^2$. The best qualitative agreement between this relation and the data in the *ab* plane at 2.5 K was achieved for magnetic layers determined by the combination of the Cu(II) ions denoted as 2, 2′, 1′ and 3, 3′, 1′ (Fig. 1). Considering the distances between the Cu(II) ions and the relative position of the magnetic $d_{x^2-y^2}$ orbitals, the layer 3, 3′, 1′ has been chosen for further analysis. Accordingly, Eq. (7) is modified to

$$\Delta B = A^* + B^*\cos^2\theta + C^*[3\cos^2\theta_{\mathrm{m}}(\Gamma + \delta') - 1]^2, \tag{8}$$

where the angle δ' was added to include a possible deviation due to the crystal misorientation or other sources.

From the fit [Fig. 5(a)] we found a nearly temperature-independent shift $\delta' \approx 13^\circ$. This value roughly corresponds to the deviation of the monoclinic angle from 90°. The increase of the parameters A^* and C^* towards lower temperatures might be associated with the growth of short-range magnetic correlations. The opposite temperature dependence of the parameter B^* that is dominated by contributions from spin anisotropies is expected by theory.[38] At high temperatures, the $(3\cos^2\theta_{\mathrm{m}}\text{-}1)^2$ term vanishes, which may be related to a strong overlap with the spin-anisotropy contributions enhanced at higher temperatures and to structural changes indicated by our neutron studies. The increase of the *c* lattice parameter (Fig. 2, inset) could interfere with the formation of the two-dimensional magnetic correlations due to the weakening of the exchange coupling between the Cu-spin pairs (3, 3′) and (3, 1′) at higher temperatures [Fig. 1(b)].

The temperature dependence of the EPR linewidth has been investigated for fields applied along the *a* and *b* axes (Fig. 6). For both orientations, the linewidth is characterized by a slight linear decrease down to about 100 K followed by an upturn for the *b* direction, while the linewidth for the *a* direction remains nearly constant; a slight upturn appears here below 10 K. The broadening at low temperatures can be associated with the development of intralayer magnetic correlations. Theoretical studies of 2D magnets showed that the formation of short-range order results in a broadening that qualitatively can be described by a $1/\chi T$ dependence.[37] As can be seen from Fig. 6, both upturns follow a $1/\chi_p T$ dependence, where χ_p is the powder susceptibility taken from Ref. 18.

The linear dependence of the linewidth develops at temperatures comparable to the average value of Debye temperature θ_{D} ≈160 K calculated from the low-temperature lattice specific heat of Cu(*en*)$(H_2O)_2SO_4$, estimated in Ref. 27. Such a linear

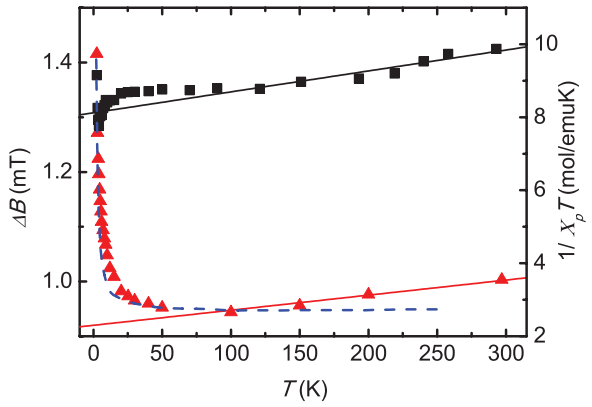

FIG. 6. (Color online) Temperature dependence of the EPR linewidth for magnetic fields applied along the a (squares) and b (triangles) axes. The solid lines represent fits to Eq. (9) and the dashed line corresponds to $1/\chi_p T$.

increase in low-dimensional Cu(II)-based magnetic systems has been ascribed to a modulation of the spin anisotropies by phonons.[40,41] The high-temperature linewidth can be described by

$$\Delta B = Q + PT, \tag{9}$$

where $P = P_S + P_A$. P_S and P_A represent the contributions of the phonon modulation of the symmetric anisotropic and antisymmetric exchange, respectively. The parameter Q corresponds to the second moment in the asymptotic regime $M_2(J/k_BT \to 0)$, which can be expressed via the microscopic spin-Hamiltonian parameters. From the fit using the data for the field aligned along the b direction, we obtain $Q = 0.9$ mT and $P = 2.75 \times 10^{-4}$ mT/K. Following Ref. 40, the asymptotic value of the second moment for a Lorentzian lineshape is given by

$$\frac{M_2}{(g\mu_B)^2} = \frac{2QH_{ex}}{zS\pi}, \tag{10}$$

where H_{ex} is the exchange field, z is a number of nearest neighbors, and $S = 1/2$. Using $z = 4$ and $J/k_B = 2.8$ K, we obtain $M_2^b/(g\mu_B)^2 \cong 1170$ mT^2. An explicit calculation of the dipolar contribution to M_2 has been performed in Ref. 28, yielding $M_2^{dip}/(g\mu_B)^2 \cong 265$ mT^2. Apparently, the asymptotic value of the second moment is dominated by other, more significant broadening contributions.

Theoretical studies of the line broadening due to spin-anisotropy effects[40] gave the asymptotic value of the second moment $M_2 \approx 2/3zS(S+1)K^2$, where the parameter K reflects the strength of the total spin anisotropy. After the subtraction of the dipolar contribution from $M_2^b, K^b/g\mu_B \approx 20$ mT was evaluated. Moriya's estimate of the strength of the antisymmetric exchange, $d \approx (\Delta g/g)J$, yields $d/g\mu_B \approx 60$ mT for $\Delta g = g_b - g, g_b \approx 2.06$ and $g = 2$. Since the symmetric anisotropic exchange is two orders of magnitude smaller, the main contribution to the line broadening in the asymptotic regime can be ascribed to the antisymmetric exchange.

For fields aligned along the a direction, we obtain $Q = 1.3$ mT and $P = 3.8 \times 10^{-4}$ mT/K. With Eq. (10), we estimate $M_2^a/(g\mu_B)^2 \cong 1660$ mT^2 and $K^a/g\mu_B \approx 26$ mT, while $d/g\mu_B \approx 280$ mT, when $\Delta g = g_a - g$ and $g_a \approx 2.28$. Given that the magnetic layer can be formed by the Cu(II) ions denoted as 3, 3′, 1′ (Fig. 1), the exchange coupling and, correspondingly, the antisymmetric exchange should be absent along the a direction. Then, the main contribution to the asymptotic line broadening is caused by the spin anisotropy induced by dipolar coupling J^{DD}, which in Cu(en)$(H_2O)_2SO_4$ is of the order $(\Delta g/g)^2 J$ and equals to $J^{DD}/g\mu_B \approx 40$ mT. The temperature dependence of the linewidth along the a axis is consistent with the theoretical prediction for the second moment of a symmetric anisotropic exchange calculated for a ferromagnet on a square lattice.[38]

Concerning the slope of the linewidth P both contributions P_S and P_A vary as $J^4 \cdot \lambda^2/\nu^5$ where λ and ν represent spin-orbit coupling and the phonon velocity, respectively.[41] The slight anisotropy of the slopes $P^a/P^b \approx 1.4$ can be ascribed to the anisotropy of elastic properties as well as the dominance of different kind of spin anisotropies along the a and b directions. The average value of the slope divided by J^4, $P/J^4 \approx 5 \times 10^{-6}$ mT/K^5, is very close to the values experimentally observed in two-dimensional copper(II)-bromide salts, for which the phonon modulation of the spin anisotropies as the main source for the line broadening at high temperatures was reported.[41]

D. Magnetization and static susceptibility

The magnetic-field dependence of the magnetization of Cu(en)$(H_2O)_2SO_4$ has been studied at $T = 2$ K in magnetic fields applied along the a, b, and b' directions (inset of Fig. 7). Corrections due to the sample shape are negligible. The magnetization is linear with a slight upward curvature above 2 T. The observed anisotropy in the magnetization coincides with the g-factor anisotropy extracted from the EPR and static-susceptibility data. Analyzing the susceptibility (Fig. 7) by use of Curie-Weiss law yields the g factors, $g_a = 2.12$, $g_b = 1.96$, $g_{b'} = 2.01$, and the paramagnetic Curie temperatures $\theta_a = -2.4$ K, $\theta_b = -2.7$ K, and $\theta_{b'} = -2.9$ K. These temperatures correspond directly to the exchange coupling constants J_a, J_b, and $J_{b'}$.

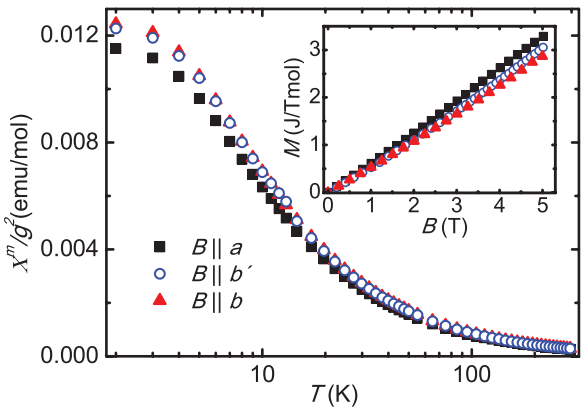

FIG. 7. (Color online) Temperature dependence of the corrected molar static susceptibility χ^m/g^2 in the field 1 T applied along the a, b, and b' directions. Inset: Magnetic-field dependence of the magnetization for the magnetic fields applied along the a, b, and b' directions at 2 K.

The anisotropy of the g factors is of easy-axis type with the largest value along the a axis. An easy-plane anisotropy of the exchange coupling with the lowest value of J along the a axis is evident also in the susceptibility corrected for the g-factor anisotropy (Fig. 7). The result qualitatively coincides with the exchange anisotropy found from the analysis of the resonance fields in Sec. III B. A coexistence of two anisotropies was found in a series of quasi-two-dimensional Cu(II)-pyrazine antiferromagnets where EPR spectra show an easy-axis anisotropy of the g factor, while an easy-plane anisotropy was observed in the corrected molar susceptibilities $\chi_i^{\mathrm{m}}/g_i^2$ $(i = x, y, z)$ in the vicinity of the ordering temperature.[23]

Recently, the role of the exchange anisotropy, antisymmetric exchange, and g-factor anisotropy in the ground-state properties of low-dimensional and geometrically frustrated magnets was investigated theoretically.[11,14,42,43] One of the criteria reflecting the resulting anisotropy is the ratio of the uniform susceptibilities $\chi_z/\chi_{x,y}$ depending on the magnetic lattice and the type of spin anisotropy. The estimate of this ratio has been used as a main tool for the experimental determination of the spin anisotropy in the spin-1/2 Kagomé antiferromagnet $ZnCu_3(OH)_6Cl_2$ with spin-liquid ground state.[44] The analysis revealed $\chi_z/\chi_{x,y} < 1$ and the result led to the conclusion of the presence of an easy axis. For Cu(*en*)$(H_2O)_2SO_4$, the ratio of the uniform susceptibilities was evaluated using the relation between the experimental (molar) susceptibility and the uniform susceptibility $\chi_i = \chi_i^{\mathrm{m}} k_B J_i/(N_A g_i^2 \mu_B^2)$, $(i = a, b, b')$ with the g factors and J's as found from the Curie-Weiss analysis stated above. The ratio $\chi_a/\chi_{b'}$ is very close to 0.84 in the whole temperature range and the average value of χ_a/χ_b is 0.91. Considering calculations of the uniform susceptibility performed for Kagomé and square-lattice antiferromagnets with spin anisotropy,[14,42] ratios values smaller than 1 suggest the prevalence of an easy-axis anisotropy in Cu(*en*)$(H_2O)_2SO_4$.

The variation of the J's extracted from the susceptibility data is of the order $(\Delta g/g)J$ which suggests that the anisotropy might be introduced by antisymmetric DM coupling. The rather large difference in the exchange anisotropies obtained from the analysis of the resonance fields and the magnetic susceptibility might be ascribed to an interplay of the spin anisotropies and demagnetizing field resulting in a shift of the resonance fields.[45] An overlap of the DM anisotropy with easy-axis anisotropy was suggested in the two-dimensional antiferromagnet $K_2V_3O_8$ (Ref. 46). The effect of DM anisotropy can be amplified by an external magnetic field which introduces spin gaps in the excitation spectra.[47] In this context, further experimental studies of Cu(*en*)$(H_2O)_2SO_4$ at low temperatures are necessary for a better understanding of the spin anisotropy.

IV. CONCLUSION

We studied in detail the spin anisotropy in Cu(*en*)$(H_2O)_2SO_4$ by use of EPR, magnetization and static-susceptibility measurements. The largest g factor and the smallest exchange coupling has been found along the a axis. The effective exchange anisotropy is of the order $(\Delta g/g)^2 J$ and originates from the dipolar anisotropy, which is the main broadening mechanism of the EPR signal along the a axis, while the DM interaction dominates the broadening along the b axis. The spin anisotropies determine the high-temperature EPR spectra. The occurrence of spin-diffusion effects at lowest temperatures in the ab plane enabled the identification of the potential magnetic layer. In this context, the vanishing of these spin-diffusion effects at higher temperatures could be associated with structural changes as observed by powder neutron diffraction.

The exchange and g-factor anisotropies obtained from the EPR spectra was confirmed by the susceptibility data. The ratio of the uniform susceptibilities and the anisotropies of the g factor and exchange coupling suggest an easy-axis anisotropy in Cu(*en*)$(H_2O)_2SO_4$. This anisotropy could govern the phase transition to the ordered state in zero magnetic field and might explain the observation of the λ-like anomaly in the specific heat. In applied magnetic fields aligned along the a axis a crossover between the intrinsic easy-axis anisotropy and a field-induced easy-plane anisotropy should appear. Experimental studies of the magnetic phase diagram in the quasi-two-dimensional $[Cu(pyz)_2(pyO)_2](PF_6)_2$ antiferromagnet showed that the interplay of the intrinsic spin anisotropy and the applied field results in a variety of physical properties depending on the orientation of the magnetic field.[48]

The determination of the magnetic structure in the ordered phase is another issue. The present analysis of the spin anisotropy suggests an antiferromagnetic ordering with the main component of the magnetic moments along the a axis. A significant reduction of the order parameter due to frustration has been reported for the collinear Néel phase of SATL antiferromagnets.[10,49] Thus, the determination of the magnetic moments could provide some information about the degree of frustration in Cu(*en*)$(H_2O)_2SO_4$.

In this context, theoretical studies of SATL with a weak easy-axis anisotropy would be desirable to determine a ground-state phase diagram as well as the order parameter.

ACKNOWLEDGMENTS

The authors are grateful to M. W. Meisel for useful discussions. The technical support of K. Kiefer and S. Gerischer from Helmholtz-Zentrum Berlin is acknowledged. This work was supported by CFNT MVEP—Centre of Excellence of SAS and the projects APVV LPP-0202-09, VEGA 1/0143/13, Deutsche Forschungsgemeinschaft, EuroMagNET (EU Contract No. 228043), 7FP CP-CSA-INFRA-2008-1.1.1 Number 226507-NMI3 and ERDF EU Grant No. ITMS26220120005. Material support from U.S. Steel Košice s.r.o. is greatly acknowledged.

*alzbeta.orendacova@upjs.sk

[1] L. Balents, Nature (London) **464**, 199 (2010).

[2] U. Schollwöck, J. Richter, D. J. J. Farnell, and R. F. Bishop, *Quantum Magnetism* (Springer-Verlag, Berlin, 2004).

[3] R. Coldea, D. A. Tennant, A. M. Tsvelik, and Z. Tylczynski, Phys. Rev. Lett. **86**, 1335 (2001).

[4] M. Q. Weng, D. N. Sheng, Z. Y. Weng, and R. J. Bursill, Phys. Rev. B **74**, 012407 (2006).

[5]S. Yunoki and S. Sorella, Phys. Rev. B **74**, 014408 (2006).
[6]P. Hauke, T. Roscilde, V. Murg, J. I. Cirac, and R. Schmied, New J. Phys. **13**, 075017 (2011).
[7]Y. Nishiyama, Phys. Rev. B **79**, 054425 (2009).
[8]R. F. Bishop, P. H. Y. Li, D. J. J. Farnell, and C. E. Campbell, Phys. Rev. B **79**, 174405 (2009).
[9]K. Harada, Phys. Rev. B **86**, 184421 (2012).
[10]L. O. Manuel and H. A. Ceccatto, Phys. Rev. B **60**, 9489 (1999).
[11]P. Hauke, T. Roscilde, V. Murg, J. I. Cirac, and R. Schmied, New J. Phys. **12**, 053036 (2010).
[12]O. A. Starykh and L. Balents, Phys. Rev. Lett. **98**, 077205 (2007).
[13]O. A. Starykh, H. Katsura, and L. Balents, Phys. Rev. B **82**, 014421 (2010).
[14]A. Cuccoli, T. Roscilde, V. Tognetti, R. Vaia, and P. Verrucchi, Phys. Rev. B **67**, 104414 (2003).
[15]G. H. Wannier, Phys. Rev. **79**, 357 (1950).
[16]P.-É. Melchy and M. E. Zhitomirsky, Phys. Rev. B **80**, 064411 (2009).
[17]H. D. Zhou, C. Xu, A. M. Hallas, H. J. Silverstein, C. R. Wiebe, I. Umegaki, J. Q. Yan, T. P. Murphy, J.-H. Park, Y. Qiu, J. R. D. Copley, J. S. Gardner, and Y. Takano, Phys. Rev. Lett. **109**, 267206 (2012).
[18]M. Kajňaková, M. Orendáč, A. Orendáčová, A. Vlček, J. Černák, O. V. Kravchyna, A. G. Anders, M. Balanda, J.-H. Park, A. Feher, and M. W. Meisel, Phys. Rev. B **71**, 014435 (2005).
[19]L. Sedláková, Ph.D. Thesis, P. J. Šafárik University, Košice, 2010.
[20]A. Cuccoli, T. Roscilde, R. Vaia, and P. Verrucchi, Phys. Rev. B **68**, 060402(R) (2003).
[21]P. Sengupta, C. D. Batista, R. D. McDonald, S. Cox, J. Singleton, L. Huang, T. P. Papageorgiou, O. Ignatchik, T. Herrmannsdörfer, J. L. Manson, J. A. Schlueter, K. A. Funk, and J. Wosnitza, Phys. Rev. B **79**, 060409(R) (2009).
[22]P. Sengupta, A. W. Sandvik, and R. R. P. Singh, Phys. Rev. B **68**, 094423 (2003).
[23]F. Xiao, F. M. Woodward, C. P. Landee, M. M. Turnbull, C. Mielke, N. Harrison, T. Lancaster, S. J. Blundell, P. J. Baker, P. Babkevich, and F. L. Pratt, Phys. Rev. B **79**, 134412 (2009).
[24]V. Manríquez, M. Campos-Valette, N. Lara, N. González-Tejeda, O. Wittke, G. Díaz, S. Diez, R. Muñoz, and L. Kriskovic, J. Chem. Crystall. **26**, 15 (1996).
[25]T. Moriya, Phys. Rev. **120**, 91 (1960).
[26]J. Rodríguez-Carvajal, Physica B **192**, 55 (1993).
[27]L. Sedláková, R. Tarasenko, I. Potočňák, A. Orendáčová, M. Kajňaková, M. Orendáč, V. A. Starodub, A. G. Anders, O. Kravchyna, and A. Feher, Solid State Commun. **147**, 239 (2008).
[28]O. V. Kravchina, A. I. Kaplienko, E. P. Nikolova, A. G. Anders, D. V. Ziolkovskij, A. Orendachova, and M. Kajnakova, Russian J. Phys. Chem. B **5**, 209 (2011).
[29]S. Brown, J. Cao, J. L. Musfeldt, M. M. Conner, A. C. McConnel, H. I. Southerland, J. L. Manson, J. A. Schlueter, M. D. Phillips, M. M. Turnbull, and C. P. Landee, Inorg. Chem. **46**, 8577 (2007).
[30]I. Yamada, M. Nishi, and J. Akimitsu, J. Phys.: Condens. Matter **8**, 2625 (1996).
[31]H.-A. Krug von Nidda, L. E. Svistov, M. V. Eremin, R. M. Eremina, A. Loidl, V. Kataev, A. Validov, A. Prokofiev, and W. Aßmus, Phys. Rev. B **65**, 134445 (2002).
[32]R. Calvo and M. C. G. Passeggi, Phys. Rev. B **44**, 5111 (1991).
[33]K. Nagata, I. Yamamoto, H. Takano, and Y. Yokozawa, J. Phys. Soc. Jpn. **43**, 857 (1977).
[34]K. Nagata and Y. Tazuke, J. Phys. Soc. Jpn. **32**, 337 (1972).
[35]K. T. McGregor and Z. G. Soos, J. Chem. Phys. **64**, 2506 (1976).
[36]R. D. Willett, F. H. Jardine, I. Rouse, R. J. Wong, Ch. P. Landee, and M. Numata, Phys. Rev. B **24**, 5372 (1981).
[37]P. M. Richards and M. B. Salamon, Phys. Rev. B **9**, 32 (1974).
[38]Z. G. Soos, K. T. McGregor, T. T. P. Cheung, and A. J. Silverstein, Phys. Rev. B **16**, 3036 (1977).
[39]M. Herak, A. Zorko, D. Arčon, A. Potočnik, M. Klanjšek, J. van Tol, A. Ozarowski, and H. Berger, Phys. Rev. B **84**, 184436 (2011).
[40]T. G. Castner, Jr. and M. S. Seehra, Phys. Rev. B **4**, 38 (1971).
[41]R. D. Willett and R. J. Wong, J. Magn. Reson. **42**, 446 (1981).
[42]M. Rigol and R. R. P. Singh, Phys. Rev. B **76**, 184403 (2007).
[43]K. V. Tabunshchyk and R. J. Gooding, Phys. Rev. B **71**, 214418 (2005).
[44]T. Han, S. Chu, and Y. S. Lee, Phys. Rev. Lett. **108**, 157202 (2012).
[45]J. L. Stanger, J. J. André, P. Turek, Y. Hosokoshi, M. Tamura, M. Kinoshita, P. Rey, J. Cirujeda, and J. Veciana, Phys. Rev. B **55**, 8398 (1997).
[46]M. D. Lumsden, B. C. Sales, D. Mandrus, S. E. Nagler, and J. R. Thompson, Phys. Rev. Lett. **86**, 159 (2001).
[47]A. L. Chernyshev, Phys. Rev. B **72**, 174414 (2005).
[48]Y. Kohama, M. Jaime, O. E. Ayala-Valenzuela, R. D. McDonald, E. D. Mun, J. F. Corbey, and J. L. Manson, Phys. Rev. B **84**, 184402 (2011).
[49]A. E. Trumper, Phys. Rev. B **60**, 2987 (1999).